Black Holes Through a Nonsingular Cyclic Bounce

Lia Hankla
Advisor: Frans Pretorius

January 5, 2016

Contents

1 Introduction

As the study of the origin and evolution of the universe, one of cosmology's primary goals is to provide a cohesive theory of how the universe began and where it will end up. However, inflation, often considered the dominant such theory, suffers a variety of problems, to be detailed in Section 2.d, that make it appropriate to consider other, less-standard theories. The model under consideration in this work, termed the "cyclic" model, is an alternative to inflation essentially characterized by an expanding phase (a big bang), followed by a contraction (or big crunch), after which the entire universe collapses to either a singularity (a "singular bounce" cyclic model) or a finite volume (a "nonsingular bounce" cyclic model) before rebounding into another big bang and repeating the process–hence the term "cyclic". The mechanisms behind the cyclic theory will be explained in Section 3.

A major motivating factor for considering the cyclic model stems from the presence of supermassive black holes in the early universe. Quasars on the order of a billion solar masses have been dated back to a time when the universe was less than one billion years old [1], challenging the predominant theory for how these supermassive black holes formed. Said predominant theory hypothesizes that the first stars in the early universe collapsed into black holes and accreted enough matter over time to reach supermassive scales: a reasonable guess, since this is how stellar-mass black holes form. However, estimates of the masses of these initial stars vary between a few hundred solar masses to merely tens of solar masses; the lower end of the scale does not manage to create sufficiently large black holes on the time scales of the universe [2], and thus it is possible that this theory in the context of inflation would not explain the existence of observed quasars.

In this work an alternative possibility using the cyclic model as a backdrop is explored. In the cyclic model, black holes could survive from a time before the big bang, passing through a (non-singular or singular) bounce, and emerging after the big bang already with considerable mass. The goal of this paper is to study a range of black hole masses in order to predict, to zeroth-order approximation, the mass and radius profiles slightly before, during, and slightly after a cosmic bounce to see what kinds of black holes would survive a cyclic bounce. This is accomplished by modeling accretion of two scalar fields, one a canonical matter field, the other a ghost field with negative kinetic energy (necessary for a non-singular bounce, as explained in Section 3.b), onto the black hole (the utilized accretion process in described in Section 2.c). Scalar field basics are outlined in Section 2.b.

Throughout, reduced Planck units ($8\pi G = c = 1$) are employed unless otherwise noted.

2 Background Information

This section will begin with some key concepts in cosmology, introducing the Friedmann equations and basic scalar field manipulations, and then proceed to motivate the cyclic model by exploring elements of a coherent origin theory. This section follows Chapter 8 in Carroll [3].

The method in this paper is to superimpose a black hole onto a Friedmann-Robertson-Walker (FRW) background universe (flat at any given time, but expanding), and so the metric is given by

$$ds^2 = -dt^2 + a^2(t)\left[\frac{dr^2}{1-\kappa r^2} + r^2 d\Omega^2\right] \tag{1}$$

which is hypothesized due to the requirement that space be isotropic and homogeneous. Here, t is physical time, a is the dimensionless scale factor, and κ, with dimensions of length^{-2}, takes on any value depending on the curvature of the spacetime. Current observations estimate κ as being very close to zero.

2.a Friedmann Equations

Modeling matter and energy as a perfect fluid, the fluid's 4-velocity in its rest frame is given by $U^\mu = (1,0,0,0)$ such that $U^\mu U_\mu = -1$, and the energy-momentum tensor is found by

$$\begin{aligned} T_{\mu\nu} &= (\rho + p)U_\mu U_\nu + p g_{\mu\nu} \\ T^\mu_{\ \nu} &= g^{\mu\sigma}T_{\sigma\nu} = (\rho+p)U^\mu U_\nu + p\delta^\mu_\nu \\ &= \begin{pmatrix} -\rho & 0 & 0 & 0 \\ 0 & p & 0 & 0 \\ 0 & 0 & p & 0 \\ 0 & 0 & 0 & p \end{pmatrix} \end{aligned}$$

where ρ is the fluid energy density and p is the pressure. The trace of the tensor is $T^\mu_{\ \mu} = T = -\rho + 3p$. Extending the perfect fluid analogy, an equation of state $p = w\rho$ is introduced, where, for example, $w = 0$ for dust (no pressure), $1/3$ for radiation, and -1 for a vacuum. Then, by conservation of energy,

$$\begin{aligned} 0 &= \nabla_\mu T^\mu_{\ 0} \\ &= \partial_\mu T^\mu_{\ 0} + \Gamma^\mu_{\mu\lambda} T^\lambda_{\ 0} - \Gamma^\lambda_{\mu 0} T^\mu_{\ \lambda} \end{aligned} \tag{2}$$

where $\Gamma^{\lambda}_{\mu\nu}$ is the Christoffel connection. The needed non-zero symbols are obtained via the derivable shortcut formula for a diagonal metric $\Gamma^{\lambda}_{\lambda\mu} = \partial_\mu \left(\ln \sqrt{|g_{\lambda\lambda}|} \right)$:

$$\Gamma^1_{10} = \Gamma^2_{20} = \Gamma^3_{30} = \frac{\dot{a}}{a}$$

where the dot represents the derivative with respect to physical time t. Then Equation 2 becomes

$$\begin{aligned} 0 &= \nabla_\mu T^\mu_{\ 0} \\ &= \partial_0 T^0_{\ 0} + (\Gamma^1_{10} + \Gamma^2_{20} + \Gamma^3_{30}) T^0_{\ 0} - \Gamma^1_{10} T^1_{\ 1} - \Gamma^2_{20} T^2_{\ 2} - \Gamma^3_{30} T^3_{\ 3} \\ &= -\dot{\rho} - 3\frac{\dot{a}}{a}(\rho + p) \end{aligned}$$

If w is constant, then one can integrate the conservation of energy equation, implying that

$$\rho \propto a^{-3(1+w)}$$

Thus the energy density of ordinary matter ($w = 0$) scales as a^{-3} (the energy density of matter is dominated by the rest energy, which is proportional to the number density and thus volume), radiation ($w = 1/3$) as a^{-4} (due to the same effect as matter with an additional decrease in energy due to redshifting), and the vacuum energy density is constant. Below, a scalar field with $w \gg 1$ is considered, for which the energy density scales as a power of a less than -6. This will be important in showing that this scalar field in a contracting universe will dominate over, for example, the anisotropy term.

The Friedmann equations, two of the most relevant equations to this paper, govern the background behavior of the universe. They are derived from Einstein's field equations $R_{\mu\nu} = T_{\mu\nu} - \frac{1}{2} g_{\mu\nu} T$, whose 00 (time) and ij (spatial) components supply two unique equations (the three spatial components give the same equation, since space is assumed to be isotropic). In reduced Planck units with $\kappa = 0$ for flat space, these are:

$$\left(\frac{\dot{a}}{a} \right)^2 = H^2 = \frac{\rho}{3} \tag{3}$$

$$\frac{\ddot{a}}{a} = \dot{H} + H^2 = -\frac{1}{6}(\rho + 3p) \tag{4}$$

where $H = \dot{a}/a$ is the Hubble parameter.

2.b Scalar Fields

Since this work is concerned with scalar fields, the Friedmann equations are more relevant in terms of the derivatives of the fields, rather than in terms of the fluid analogy's ρ and

p. Proceeding with the Lagrangian formalism and following [3], the action for a regular canonical scalar field ϕ is given by

$$S = \int d^4x\sqrt{-g}\left[-\frac{1}{2}g^{\mu\nu}\nabla_\mu\phi\nabla_\nu\phi - V(\phi)\right]$$

where g is the metric, d^4x the four-dimensional volume element, and V the potential for the ϕ field. The energy-momentum tensor is found by varying the action with respect to the metric and matching Einstein's equations. This paper is concerned with the equations of motion, found by the Euler-Lagrange equations for scalar fields:

$$\Box\phi - \frac{dV}{d\phi} = 0$$

where $\Box$ is the d'Alembertian. Assuming that the spatial gradient of the scalar field is 0 (isotropic space), the equation of motion is

$$\ddot{\phi} + 3H\dot{\phi} + \frac{dV}{d\phi} = 0 \tag{5}$$

Now expressing ρ and p in terms of the scalar field:

$$\rho = \frac{\dot{\phi}^2}{2} + V(\phi) \tag{6}$$

$$p = \frac{\dot{\phi}^2}{2} - V(\phi) \tag{7}$$

The Friedmann Equations are thus given by:

$$\left(\frac{\dot{a}}{a}\right)^2 = H^2 = \frac{1}{3}\left(\frac{1}{2}\dot{\phi}^2 + V\right) \tag{8}$$

$$\frac{\ddot{a}}{a} = \dot{H} + H^2 = -\frac{1}{3}\left(\dot{\phi}^2 - V\right) \tag{9}$$

These equations will be used in Section 4 to solve for the behavior of two scalar fields.

2.c Accretion

Accretion of scalar fields onto a black hole is taken to be spherically-symmetric. In this model, a non-radiating perfect fluid of uniform density and pressure accretes steadily onto a black hole in an asymptotically flat space. It is assumed that the fluid is much lighter than the black hole, such that its own effects on the metric can be neglected, and that the accretion is slow enough that the fluid's distribution adjusts to the black hole's new mass, ensuring a homogeneous spatial distribution.

Assuming the fluid falls in radially at the same rate from all directions, the black hole mass changes as

$$\dot{M} = \frac{1}{2} A M^2 (\rho + p(\rho)) \tag{10}$$

where A is a constant (equal to 4 for most fluids) and ρ and $p(\rho)$ are the energy density and pressure of the accreting fluid, respectively. In Section 4, the energy density and pressure are functions of time. A is calculated from

$$A = \frac{(1+3\alpha)^{(1+3\alpha)/2\alpha}}{4\alpha^{3/2}}$$

where α is defined through $p = \alpha(\rho - \rho_0)$, an alternative formulation of the fluid equation of state. w is related to α via $w = \alpha(\rho - \rho_0)/\rho$ [4]. For a scalar field with $w = 1$, $\alpha = 1$ and thus $A = 4$. Any difference in choice of A will result in a simple linear scaling of the accretion rate, and thus $A = 4$ is a safe choice for both fluids considered in Section 4.

An interesting, if perhaps expected, result of this formula is that the mass of the black hole decreases when $\rho + p \leq 0$, as for a ghost field. This is not a violation of the Penrose/Hawking Singularity Theorems since the NEC condition as described in Section 3.b is not met [5]. It is thus possible for a black hole going through a bounce to accrete enough of the ghost field to reach zero mass.

2.d Problems with Inflation

A theory successfully describing the origin of the universe must address the problems of homogeneity, isotropy, and flatness: that is, why is the cosmic background radiation so uniform, with nearly scale-invariant fluctuations in the density and temperature, and how could the universe have started out so extremely flat, with κ so close to zero? For comparison with the cyclic model, it is useful to first review how inflation resolves these problems and then discuss where it is lacking.

The Friedmann Equation (3) generalizes for multiple types of matter as

$$H^2 = \frac{1}{3} \sum_i \rho_i \tag{11}$$

which becomes

$$H^2 = \frac{1}{3} \left(-\frac{3\kappa}{a^2} + \frac{\rho_m}{a^3} + \frac{\rho_r}{a^4} + \frac{\sigma^2}{a^6} + ... + \rho_I \right)$$

for our universe, with κ the curvature as above, ρ_m the energy density of matter, ρ_r the radiation energy density, σ the energy density of anisotropies in the universe's curvature,

and ρ_I the inflaton, a field specific to inflation with $w \approx -1$ [6]. Potential other forms of energy/matter are accounted for in the ellipses. In an expanding universe, the inflaton eventually comes to dominate (since its energy density is roughly constant, whereas the rest of the components decrease in importance as a increases). This includes the anisotropy and curvature term, which means that the universe keeps getting flatter and more homegenous as it evolves, thereby explaining the current state of the universe [7].

Inflation predicts the observed scale-invariant fluctuations in density in that the Hubble radius $1/H$ increases faster than the scale factor a, and thus that for some period of time the Hubble radius does not change significantly. This is shown across the literature, for example in [6].

Despite these successes, many questions remain concerning inflation. For example, why is the universe so finely-tuned? How did inflation come about in the first place? In addition, due to quantum fluctuations, inflation could last forever, which is clearly not what actually happened [6]. The predictive power of inflation is thus severely reduced, and it is worth cosidering other theories, such as the cyclic model.

3 The Cyclic Model

A cyclic model of the universe is characterized by the repetition of a big bang-big crunch cycle. A big bang occurs and the universe evolves in a manner similar to the post-inflation models of today: it expands and at varying times is dominated by radiation, matter, and dark energy (Figure 1). Then, however, the universe begins to contract, in what is called the "ekpyrotic" phase (literally, "out of the fire" [6]), and eventually experiences a big crunch in which all of spacetime collapses to a finite volume (or a singular point, in a singular theory). The universe then explodes into another big bang and the process repeats itself. The point at which the universe reaches its smallest volume is termed the "bounce" and in this paper, it is assumed that the universe collapses uniformly, which may be an idealization [8].

The typical cyclic model's contracting ekpyrotic phase before the bounce has $w \gg 1$. This is unphysical at first glance, since perfect fluids have the property that $w = c_s^2$, where c_s is the speed of sound in the fluid. For $w > 1$, then, the speed of sound in a perfect fluid would be greater than 1, the speed of light. However, different interpretations are possible [6].

The cyclic model is successful at explaining the same problems as inflation due to its contracting phase. Taking

$$H^2 = \frac{1}{3}\left(-\frac{3\kappa}{a^2} + \frac{\rho_m}{a^3} + \frac{\rho_r}{a^4} + \frac{\sigma^2}{a^6} + ... + \frac{\rho_\phi}{a^{3(1+w_\phi)}}\right)$$

where $w_\phi \gg 1$, it is evident that in a contracting universe, the energy density of the scalar field ϕ comes to dominate over all other terms, including the anisotropy term and the curvature term, since $3(1 + w_\phi) > 6$, as a gets smaller. In this way, the cyclic model's ekpyrotic phase produces a flat, homogeneous, isotropic universe.

The scale-invariant density perturbations are handled by noting that, for a contracting universe, density modes are seen if $1/H$ shrinks faster than the scale factor a. This is satisfied by the ekpyrotic scalar field [6]. In this way, the cyclic model handles the same problems of flatness and homogeneity that a good theory of the universe would and can be considered a viable alternative to inflation.

3.a The Ekpyrotic Phase

The ekpyrotic phase, the period when $w \gg 1$, is essential to the smoothing of a contracting universe, parallel to how inflation smoothes an expanding universe. This contraction is driven by a scalar field rolling down a steep negative potential (Lehners [7] suggests that the potential is exponential in form): negative in order to cancel the positive kinetic energy of matter. Density fluctuations are produced during this period. Their scale-invariance is ensured by enforcing "fast roll" conditions, explaining the required steepness of the potential. After this period, assuming the scalar field's potential has a minimum to avoid a large negative vacuum energy [9]. After this period, the potential is much less restricted. This is where the universe switches from contraction to expansion (i.e., where the bounce occurs). The potential in this paper is assumed to be an exponential as in [8].

A schematic description of the ekpyrotic scalar's potential is provided in Figure 1. The ekpyrotic phase is given as a steep negative potential with $w \gg 1$, a contracting phase which is then briefly dominated by kinetic energy before the bounce. The aforementioned minimum is achieved directly before this kinetic energy phase. The scalar field rolls back along the potential during expansion, eventually reaching the convential radiation- and matter-dominated phases, as well as the current dark energy-dominated phase. More details on the other components of the cyclic model are described in [6], from which this figure was taken.

3.b Achieving a Nonsingular Bounce

In order to model a nonsingular bounce, the scale factor's time derivative $\dot{a}$ must equal zero and reverse sign to start decreasing, and thus $\dot{H}$ must be greater than zero [7]. However, combining the two Friedmann Equations (Eqns. 3 and 4) shows that

$$\dot{H} = -\frac{1}{2}(\rho + p)$$

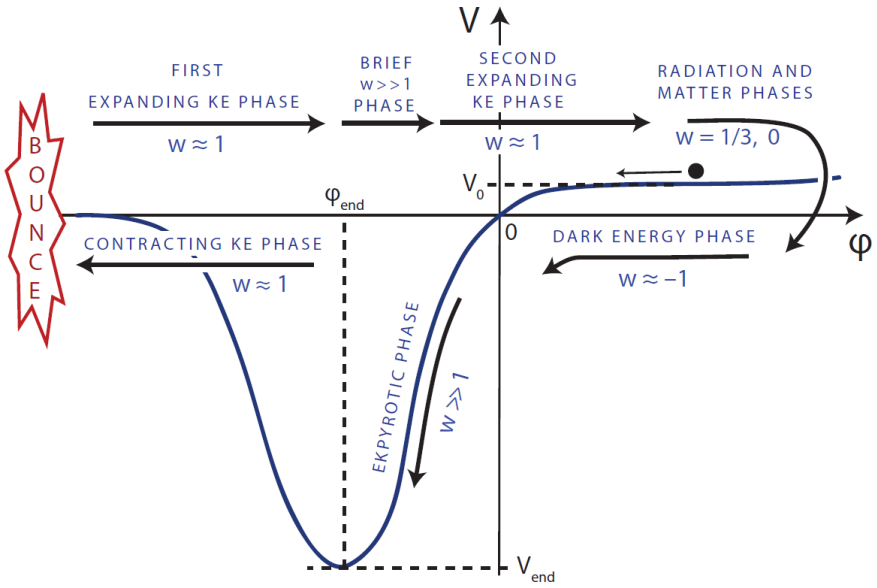

Figure 1: An example of the potential that the ekpyrotic scalar field would have. The ekpyrotic phase is steeply negative and sketches the evolution of the field over the history of the universe. V_0 is the potential energy density of the present universe. Beginning at the black dot, the future of the universe unfolds as the dot rolls to the left, eventually entering the ekpyrotic phase, encountering a bounce, and then rolling back along the curve to the right in a new cycle. Image from [6].

Therefore a positive $\dot{H}$ entails a violation of the null energy condition (NEC), which states that $\rho + p \geq 0$, implying that the energy density can be negative [3]. Usually, violation of the NEC entails ghosts and other instabilities; however, these effects can be avoided with the inclusion of higher-derivative kinetic energy terms [9].

Violation of the NEC is achieved by introducing a "ghost" field, or ghost condensate, a scalar field with negative kinetic energy, whose energy density becomes equal to that of the regular matter field at the time of the cyclic bounce. Buchbinder [9] suggests that this ghost field is also the driving scalar field behind the ekpyrotic phase, although this is irrelevant in Section 4's investigation, where only the time period around the bounce is considered. More details on what occurs near the bounce are outlined in Section 4.

Equations 6 and 7 are given for a ghost field χ as

$$\rho_\chi = -\frac{\dot{\chi}^2}{2} + V(\chi) \tag{12}$$

$$p_\chi = -\frac{\dot{\chi}^2}{2} - V(\chi) \tag{13}$$

as per Sami [10].

4 Black Hole Accretion Through a Nonsingular Bounce

The main purpose of this paper is to demonstrate what happens to black holes that go through a nonsingular cyclic bounce. Having introduced the necessary background information, the elements of scalar field behavior, black hole accretion, and cyclic bounce conditions are now combined.

A black hole is placed in a spacetime with flat spatial cross-sections (Friedmann-Robertson-Walker, as presented in Equation 1) with two scalar fields: a ghost condensate necessary to make the bounce happen, and a regular matter field representing the normal matter/energy in the universe. This approach is similar to that in [8], although the present paper's calculations are in physical instead of harmonic time (the conversion factor is given by $dt = a^3 d\tau$, where τ is harmonic time). As mentioned in Section 3.b, a violation of the NEC is unstable without higher-order kinetic terms. However, these higher-order terms are numerically unstable, demanding a simplification to two canonical scalar fields.

4.a Set-up

We consider only the time period directly before and directly after the nonsingular bounce, adopting a canonical matter field ϕ and a ghost condensate (labeled χ), a non-interacting (zero potential) scalar field with a negative kinetic energy $K = -\frac{1}{2}\nabla_\mu\chi\nabla_\mu\chi = -\frac{1}{2}(\partial\chi)^2$, whose energy density compared to that of the canonical matter field ϕ is negligible except near the bounce. Its equation of state is constant: $w_\chi = 1$.

Evolution Equations

The Lagrangian density for the combination of this ghost field and the regular matter field is given by

$$\mathcal{L} = -\frac{1}{2}(\partial\phi)^2 - V(\phi) + \frac{1}{2}(\partial\chi)^2$$

where $V(\phi)$ is the potential of the canonical field, whose shape can be taken as, for example, $V(\phi) = V_0 e^{-c\phi}$ (V_0 and c being adjustable parameters). Then the equations of motion from

Equation 5 and the equivalent for χ (with $V(\chi) = 0$) are:

$$\ddot{\phi} + 3H\dot{\phi} + \frac{dV}{d\phi} = 0$$
$$\ddot{\chi} + 3H\dot{\chi} = 0 \tag{14}$$

The generalized Friedmann equations 8 and 9 are given by

$$\frac{\ddot{a}}{a} = \dot{H} + H^2 = -\frac{1}{3}\left(\dot{\phi}^2 - V - \dot{\chi}^2\right) \tag{15}$$
$$\left(\frac{\dot{a}}{a}\right)^2 = H^2 = \frac{1}{3}\left(\frac{1}{2}\dot{\phi}^2 + V - \frac{1}{2}\dot{\chi}^2\right) \tag{16}$$

Taking after [8], we take $c = \sqrt{3}$, that of a matterlike equation of state for ϕ (then $w_\phi = c^2/3 - 1 = 0$), $V_0 = .1$, and initial conditions

$$\begin{array}{ll} \phi_0 = 0 & \dot{\phi}_0 = -\sqrt{\frac{2c^2V_0}{6-c^2}} \\ \chi_0 = 0 & \dot{\chi}_0 = \sqrt{\frac{12V_0}{(6-c^2)r_0}} \\ a_0 = 1 & H_0 = -\sqrt{\frac{2V_0(r_0-1)}{(6-c^2)r_0}} \end{array}$$

where $r_0 = 1000$ is the initial value of the ratio of the energy densities $r = |\rho_\phi/\rho_\chi|$. Solving Equations 14 and 15 numerically with Equation 16 as a constraint using Mathematica's Adams predictor-corrector method [11] yields the background behavior of a, ϕ, and χ.

The background solutions of the scale factor and ratio of the ghost field energy density to the matter field energy density are shown in Figures 2 and 3, respectively and match the results of [8] when in harmonic time.

A black hole is superimposed onto this background by generalizing Equation 10:

$$\dot{M} = 2M(t)^2\left(\dot{\phi}^2 - \dot{\chi}^2\right) = K(t)M(t)^2 \tag{17}$$

after setting $A = 4$ for both fields and using $p_\chi = \rho_\chi = -\dot{\chi}^2/2$ and $p_\phi + \rho_\phi = \dot{\phi}^2$ from Equations 6, 7, 12, and 13, where $K(t) = 2\left(\dot{\phi}^2 - \dot{\chi}^2\right)$. The evolution of black hole mass is found by solving this equation in the context of the background behavior of ϕ and χ. The resulting behavior of $K(t)$ is shown in Figure 4.

Background Scale Factor Evolution

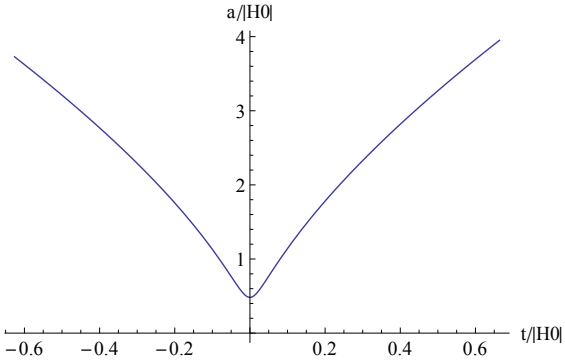

Figure 2: Time has been shifted such that the bounce occurs at $t = 0$ and scaled in units of $1/|H_0|$.

Background Energy Density Ratio

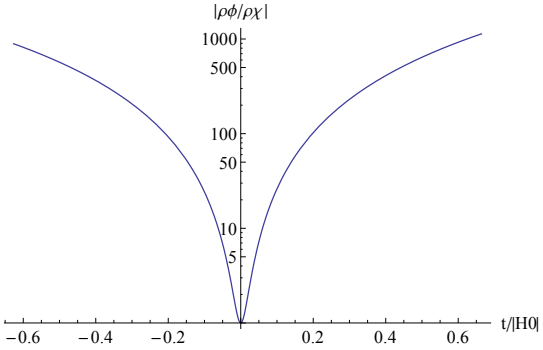

Figure 3: Time is shifted in the same way as Figure 2. The energy densities are equal ($|\rho_\phi/\rho_\chi| = 1$) at the bounce.

Evolution of $K(t)$

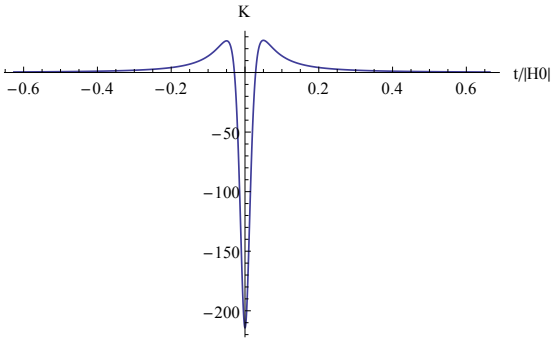

Figure 4: $K(t) = 2\left(\dot{\phi}^2 - \dot{\chi}^2\right)$. Time is scaled/shifted as before.

Black Hole Initial Mass Range

In selecting the range of black hole masses to examine, the singularity of infinite mass resulting from the solution of Equation 17 at any given time t must be avoided. Integrating the equation $\dot{M} = KM^2$ from t_0 to t and assuming K is constant during this time interval (an approximation that breaks down if the accretion onto the black hole is too fast) yields

$$M(t) = \frac{M_0}{1 - M_0 K * (t - t_0)}$$

where M_0 is the initial mass at $t = t_0$. The singularity occurs at time t_*

$$t_* = t_0 + \frac{1}{M_0 K}$$

For negative values of K (as happens near the bounce according to Figure 4), $t_* - t_0$ is also negative and the singularity occurs before the start of the simulation. Noting that we want the time of the singularity t_* to happen much later than the end of the simulation (say, t_s) for any value of K and that

$$\frac{1}{M_0 K} \geq \frac{1}{M_0 K_{max}}$$

where K_{max} is the maximum (positive) value of K, requires that

$$t_s \ll \frac{1}{M_0 K_{max}} + t_0$$

Calling $t_c = 1/M_0 K_{max}$ ($t_0 = 0$ in unscaled/unshifted time) and converting to shifted and scaled time τ_c:

$$M_0 = \frac{1}{t_c K_{max}} = \frac{1}{K_{max}\left(\frac{\tau_c}{|H_0|} + t_b\right)}$$

where t_b is the time of the bounce. Substituting in known values of K_{max}, H_0, t_b, estimating $\tau_c \approx 1$ from the range of the above figures, and scaling M_0 in units of $1/|H_0|$ yields

$$M_0 \approx .15\left[\frac{1}{|H_0|}\right] \tag{18}$$

To relate the mass of the black hole to the radius, consider the area of the black hole, given by the integral of the induced volume element of the metric:

$$\begin{aligned} A &= \int \sqrt{|\gamma|} d\theta d\phi = \int R^2 \sin\theta d\theta d\phi \\ &= 4\pi R^2 \end{aligned}$$

where R is the radius of the black hole and γ is as in [3]. But for a nonrotating black hole such as this one, the irreducible mass is the same as the mass of the black hole:

$$\begin{aligned} M_{irr}^2 &= 4\pi A = (4\pi R)^2 \\ R &= \frac{M}{4\pi} \end{aligned}$$

The constraint of Equation 18 in terms of initial black hole radius is

$$R_0 \approx .013\,[1/|H_0|] \tag{19}$$

An additional, although less restrictive, constraint is due to the approximation of placing a black hole in a Friedmann-Robertson-Walker metric, which is only valid if the radius of the black hole is much smaller than the Hubble radius $1/H$. The size of the universe is governed by the scale factor $a(t)$, which is given meaning by considering it in relation to the initial Hubble parameter H_0. The black hole radius must be smaller than the Hubble radius at any given time t. This requirement is strictest for the smallest value of $1/H$, which is the initial Hubble radius since $1/H = a/\dot{a} \to \infty$ near the bounce ($\dot{a} \to 0$). Thus

a valid initial black hole radius R_0 should be much less than $1[1/|H_0|]$.

The stricter constaint of Equation 19 suggests consideration of black holes up to the order of 10^{-2} or 1% of the initial Hubble radius. Even though the approximations are only valid for initial radii much less than this magnitude, it will be interesting to see what happens at the edge of their validity. Finally, note that any black hole reaching zero mass over the course of the simulation is removed from consideration, since a black hole will not spontaneously appear after it disappears.

A lower bound on the initial mass range is given by considering the recently discovered quasar in the early universe, with a mass of approximately 12 billion solar masses [1]. With the present Hubble constant, about 70 km/s/Mpc [3], the ratio of the quasar's radius to the current Hubble radius is approximately

$$\frac{R}{1/|H_0|} \approx 10^{-9}$$

Higher values of H_0 would increase the ratio and thus this value is a good lower bound. Combined with the upper bound in Equation 19, a reasonable range for the initial radius of a black hole runs from 10^{-9} to 10^{-2} times the initial Hubble radius.

4.b Results

Fractional Change in Black Hole Mass

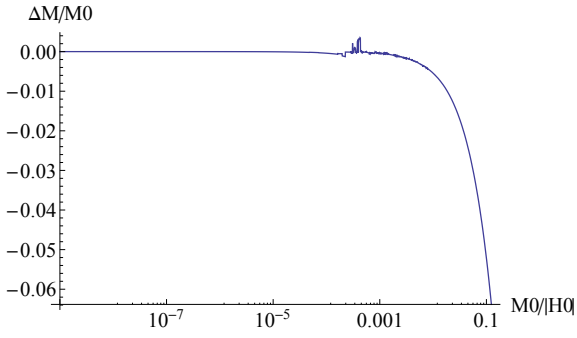

Figure 5: The fractional change in black hole mass from the time before to the time after the bounce as in Figure 6. The relationship is linear, so larger black holes lose more mass through a bounce.

All black holes that survive the bounce lose mass. Figure 5 shows the fractional change in black hole mass (change in mass divided by initial mass) of black holes with initial radii ranging from 10^{-7}% to 1% of the initial Hubble radius, beyond which the singularity of infinite mass discussed above renders the integrator's results unstable. Larger mass black holes lose more mass, but for black holes with the same initial radius as that of the quasar, the loss is on the order of 10^{-6}% of the starting mass. The perturbations around $M_0/|H_0| \approx .001$ are due to numerical rounding errors.

Due to the large range of possible initial black hole radii, only a representative selection of curves is shown in Figure 6. This figure shows evolution of black holes with initial

radii anywhere between 0 and 1% of the initial Hubble radius. Larger black holes' radii increase rapidly right before the bounce and decrease rapidly right afterwards. Lower mass black holes, notably those in the range where the approximations made are most valid, do not experience any significant change in radius through the bounce. This is because the accretion rate depends on the square of the mass. The asymmetry about the bounce is due to the dominance of the ghost field only around the bounce, which causes the black hole mass to be less at the time of the bounce than initially. Immediately after the bounce, the development is the same only with a lower starting mass and hence a lower dip (due to the accretion rate's dependency on the squared mass) which is why the dip after the bounce is less predominant than the peak before the bounce.

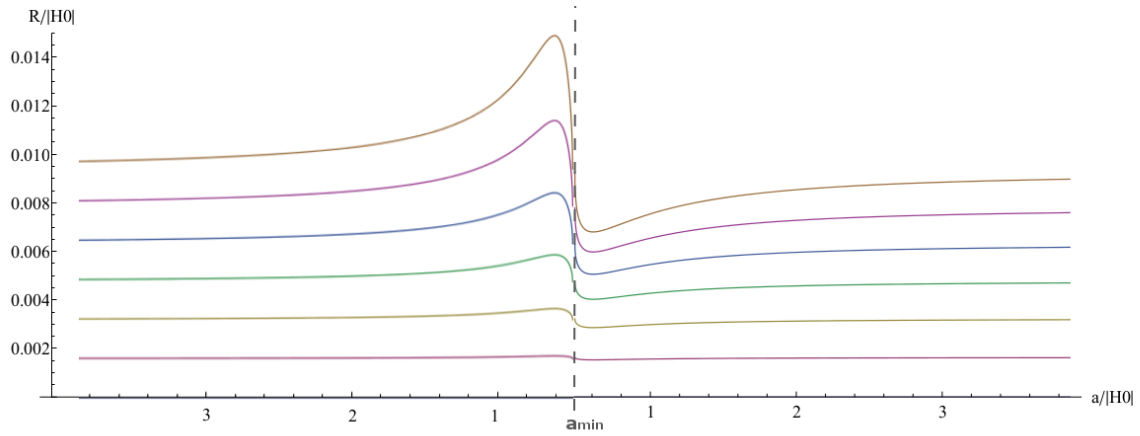

Figure 6: A profile of black hole radius as a function of scale factor before (left) and after (right) the bounce. The scale factor a has been scaled to the inital Hubble radius and reaches a minimum value a_{min} of about half the initial Hubble radius. Time proceeds monotonically (although not linearly) from left to right: the universe is collapsing to the left of a_{min} and expanding to the right. Initial radii are, from top to bottom, 1%, .8%, .66%, .49%, .33%, and .17% of the initial Hubble radius.

5 Conclusions

Interestingly, no black holes reach zero mass passing through the bounce, meaning that black holes from a previous cycle of the universe could survive through a cosmic bounce and thus explain the supermassive black holes of the early universe. Although larger black holes lose more mass than smaller black holes, they could still appear in the early universe with a significant mass, accreting matter sooner and faster than black holes that form from the first stars. In addition, the approximations seem to hold even up to the very limit, since the only significant difference between small and large black holes occurs when the

scale factor is less than the initial Hubble radius.

Figure 5 suggests that there would be fewer extremely large black holes after a bounce because these black holes would lose more mass than their lighter counterparts. However, those that would match to the range of black holes seen in the early universe would be almost as prevalent after the bounce as before. Thus the cyclic model's viability as an alternative to inflation is not diminished (although neither is it strengthened, as this scenario does not provide any direct evidence against inflation).

This simulation, however, is only a zeroth-order approximation. The scaling solution is not an attractor and thus depends heavily on initial conditions [8] (as fine-tuning is considered a problem with the theory of inflation, this dependency also presents a problem to the cyclic model). As previously mentioned, the accretion process is limited to a simple model of spherically symmetric accretion, one that also neglects back reaction on the metric. The test fluid is assumed to be isotropic, even though its density would change close to the black hole, and extremely light compared to the black hole [4]. And, of course, the black hole is simply placed directly on top of a Friedmann-Robertson-Walker spacetime, whereas a real black hole would distort the metric and result in more complicated behavior of ϕ and χ.

5.a Outlook

Further research could utilize the results of Afshordi [12] to find a more suitable metric (this paper even calculates the accretion rate of a black hole in said improved metric, although not in the context of the cyclic model or ghost fields). Babichev [13] suggests a perturbative correction to the metric to account for the typically-neglected back reaction (especially important when the accreting matter is not light compared to the mass of the black hole, i.e. for smaller black holes), providing the next highest level of approximation.

In addition, the other phases of the cyclic model were ignored in favor of investigating the behavior right around the bounce. However, the explicit purpose of the contracting ekpyrotic phase is to smooth out inhomogeneities in the spacetime, and thus black holes might not even be supported through this phase, resulting in not enough black holes passing through the bounce in the first place to account for the distribution in the modern/early universe [14]. If this were the case, then the cyclic model could not explain the abundance of supermassive black holes in the early universe, providing evidence against the cyclic model. Another useful experiment would thereby be to follow the evolution of black holes of a variety of initial masses through the ekpyrotic and then radiation-, matter-, and finally dark-energy-dominated phases to predict what size black holes would need to exist before a bounce in order to explain their present mass.

Many questions could be answered by a simulation tracking black holes through an entire cycle of the universe: could one calculate how many bounces must have occured in order to achieve the current black hole distribution from only stellar-mass black holes? If black holes lose or gain mass between bounces depending on their initial mass, could the current gap between stellar-mass and supermassive black holes be explained? If they consistently gain mass between bounces, could the universe end up as one large black hole? Such a simulation would require more accurate approximations but could provide an explanation for long-unresolved questions.

The cyclic model, for now, has not been disproven and it is worth exploring more in order to strengthen the case for or against inflation.

6 Acknowledgments

I would like to thank Frans Pretorius for both guiding this project and for the background information I learned in his General Relativity course this semester, as well as my dad, Allen Hankla, for his thorough proof-reading.

This paper represents my own work in accordance with University regulations.

References

[1] Xue-Bing Wu, Feige Wang, Xiaohui Fan, Weimin Yi, Wenwen Zuo, Fuyan Bian, Linhua Jiang, Ian D. McGreer, Ran Wang, Jinyi Yang, Qian Yang, David Thompson, and Yuri Beletsky. An ultraluminous quasar with a twelve-billion-solar-mass black hole at redshift 6.30. *Nature*, 518:512–516, 2015.

[2] M. Volonteri. The formation and evolution of massive black holes. *Science*, 337:544–547, 2012.

[3] Sean Carroll. *Spacetime and Geometry: An Introduction to General Relativity*. Pearson Education Limited, London, England, 2014.

[4] E. Babichev, V. Dokuchaev, and Y. Eroshenko. Black holes in the presence of dark energy. *Physics*, 56:1155–1175, 2013.

[5] E. Babichev, V. Douchaev, and Yu Eroshenko. Black hole mass decreasing due to phantom energy accretion. 2008. arxiv:gr-gc/0402089v3.

[6] Paul Steinhardt. The cyclic theory of the universe. `http://physics.princeton.edu/~steinh/vaasrev.pdf`. Accessed: 2015-10-10.

[7] Jean-Luc Lehners. Ekpyrotic and cyclic cosmology. 2009. arxiv:0806.1245v2.

[8] BingKan Xue, David Garfinkle, Frans Pretorius, and Paul Steinhardt. Nonperturbative analysis of the evolution of cosmological perturbations through a nonsingular bounce. *Physical Review D*, 88, 2013.

[9] Evgeny Buchbinder, Justin Khoury, and Burt Ovrut. New ekpyrotic cosmology. 2007. arxiv:hep-th/0702154v4.

[10] M. Sami and Alexey Toporensky. Phantom field and the fate of the universe. *Modern Physics Letters A*, 19(20):1509–1517, 2004.

[11] H. Binous, A. Bellagi, and B. Higgins. Two-step and four-step Adams predictor-corrector method. *Wolfram Demonstrations Project*, 2013.

[12] Niayesh Afshordi, Michele Fontanini, and Daniel Guariento. Horndeski meets McVittie: A scalar field theory for accretion onto cosmological black holes. 2014. arxiv:1408:5538v1.

[13] E. Babichev, V. Dokuchaev, and Yu Eroshenko. Backreaction of accreting matter onto a black hole in the Eddington-Finkelstein coordinates. 2012. arxiv:1202.2836v2.

[14] J.C.S. Neves. Are black holes in an ekpyrotic phase possible? 2015. arxiv:1509.03301v1.